Bioorganic & Medicinal Chemistry Letters 21 (2011) 110–116

Contents lists available at ScienceDirect

Bioorganic & Medicinal Chemistry Letters

journal homepage: www.elsevier.com/locate/bmcl

Application of p21 and klf2 reporter gene assays to identify selective histone deacetylase inhibitors for cancer therapy

Jason C. Wong [a,*], Lei Guo [a], Zhenghong Peng [a], Weixing Zhang [a], Nan Zhang [a], Wayne Lai [a], Zhenshan Zhang [a], Chao Zhang [a], Xiongwen Zhang [a], Shan Song [b], Desi Pan [b], Chuanming Xie [c], Jia Li [c], Zhiqing Ning [b], Xianping Lu [b], Yun He [a], Li Chen [a]

[a] Roche R&D Center (China) Ltd, 720 Cai Lun Road, Building 5, Pudong, Shanghai 201203, PR China
[b] Chipscreen Biosciences, Suite C301, PO Box 28, Research Institute of Tsinghua University, High-Tech Park, Nanshan District, Shenzhen, Guangdong 518057, PR China
[c] National Center for Drug Screening, 189 Guo Shou Jing Road, Zhangjiang High-Tech Park, Pudong, Shanghai 201203, PR China

ARTICLE INFO

Article history:
Received 21 August 2010
Revised 3 November 2010
Accepted 13 November 2010
Available online 19 November 2010

Keywords:
Histone deacetylase
Histone deacetylase inhibitor
In-cell selectivity
Reporter gene assay

ABSTRACT

Novel 2-aminoanilide histone deacetylase (HDAC) inhibitors were designed to increase their contact with surface residues surrounding the HDAC active site compared to the contacts made by existing clinical 2-aminoanilides such as SNDX-275, MGCD0103, and Chidamide. Their HDAC selectivity was assessed using p21 and klf2 reporter gene assays in HeLa and A204 cells, respectively, which provide a cell-based readout for the inhibition of HDACs associated either with the p21 or klf2 promoter. A subset of the designed compounds selectively induced p21 over klf2 relative to the clinical reference compound SNDX-275. A representative lead compound from this subset had antiproliferative effects in cancer cells associated with induction of acetylated histone H4, endogenous p21, cell cycle arrest, and apoptosis. The p21- versus klf2-selective compounds described herein may provide a chemical starting point for developing clinically-differentiated HDAC inhibitors for cancer therapy.

ε-Amino lysine acetylation/deacetylation is mediated, respectively, by histone acetyltransferases (HATs) and the Zn^{2+}-dependent hydrolases known as histone deacetylases (HDACs). This post-translational modification is an important modulator of protein function[1–5] that influences a number of biological processes, such as transcription,[6] the cell cycle,[7] apoptosis,[7] and differentiation.[8] In particular, inhibition of lysine deacetylation by small-molecule inhibitors of HDACs can cause cell cycle arrest, apoptosis, and/or induce differentiation depending on cellular context.[8,9] Because of their pharmacological properties, several HDAC inhibitors are being evaluated in the clinic as anticancer agents, and two compounds, SAHA and FK228, have already been approved by the FDA for the treatment of cutaneous T-cell lymphoma (Fig. 1).

The HDAC family of enzymes can be divided into two major groups, the Rpd3/Hda1-like NAD-independent lysine deacetylases and the NAD-dependent sirtuins.[10] The Rpd3/Hda1-like deacetylase group has been further organized into class I enzymes (HDACs 1, 2, 3, and 8) and class II enzymes (HDACs 4, 5, 6, 7, 9, 10) based on sequence similarity to the yeast HDACs Rpd3 and Hda1, respectively.[11] With the possible exception of HDAC8, both the class I and class II HDACs generally function as part of multiprotein complexes and apparently depend on their protein complex partners for recruitment and enzymatic activity toward their various cellular substrates.[11,12]

Many of the HDAC inhibitors currently in clinical development were identified and optimized through HDAC enzyme inhibition assays and antiproliferative functional assays.[13] In order to identify novel chemical starting points for clinically-differentiated HDAC inhibitors, we elected to employ a relatively unique combination of cell-based assays in contrast to the more traditional enzyme inhibition and cell proliferation assays. In particular, based on the link between HDAC inhibitor-induced upregulation of the cyclin dependent kinase inhibitor protein p21 and their antiproliferative effects in a variety of cancer cell lines,[9] we established a p21 reporter gene assay in HeLa cells (human cervical cancer) using a p21 promoter-luciferase construct containing only the Sp1/Sp3 binding site and not the upstream p53 binding site (Fig. 2a).[15,16] At the same time, we reasoned that induction of myocyte enhancing factor (MEF)-regulated genes (e.g., muscle growth and differentiation genes) via non-selective inhibition of its associated HDAC complex could be an undesirable pharmacological effect for an HDAC inhibitor used in cancer therapy. Therefore, we established a klf2 reporter gene assay in A204 cells (human rhabdomyosarcoma) using a klf2 promoter-luciferase construct containing the MEF binding site, based on literature reports on the regulation of klf2 expression by MEF–recruited HDAC complexes (Fig. 2b).[17] Both assay systems were generated via transient transfection using GFP to control for

* Corresponding author. Tel.: +86 21 38954910; fax: +86 21 50790292.
E-mail addresses: jason.wong@roche.com, jwong@alum.mit.edu (J.C. Wong).

0960-894X/$ - see front matter © 2010 Elsevier Ltd. All rights reserved.
doi:10.1016/j.bmcl.2010.11.063

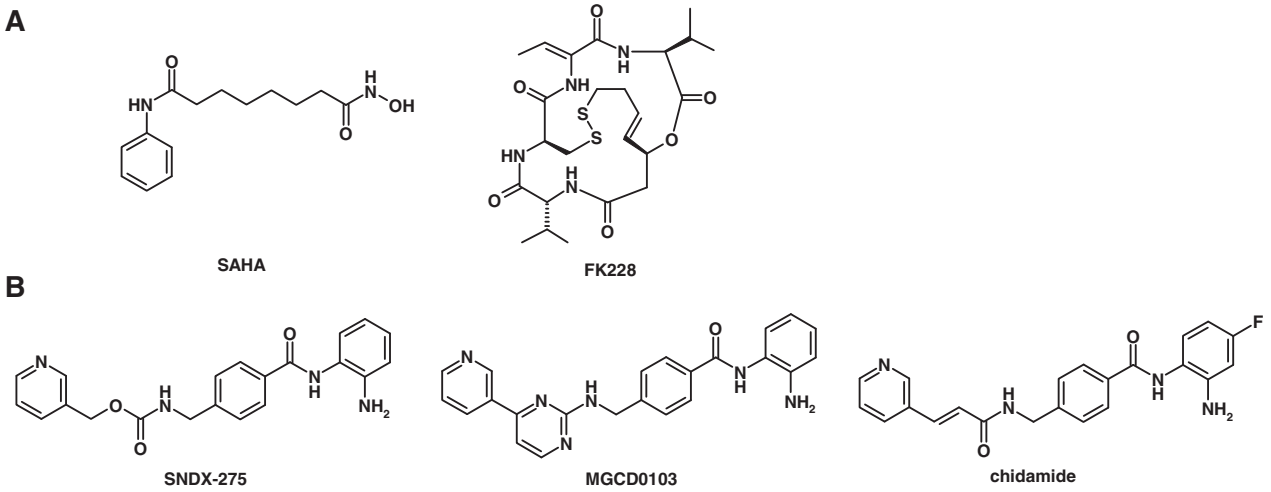

Figure 1. Selected HDAC inhibitors: (A) approved for CTCL (SAHA, FK228); (B) under clinical development (SNDX-275, MGCD0103, chidamide).

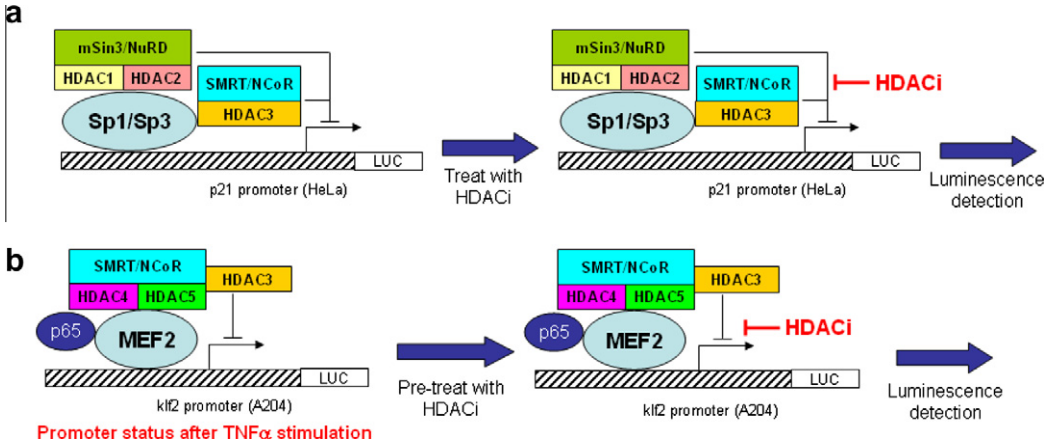

Figure 2. Assay design for (a) p21 reporter gene and (b) klf2 reporter gene, based upon reported molecular biology studies.[15–17] HDAC4&5 in this context are adaptor proteins for the active deacetylase HDAC3.

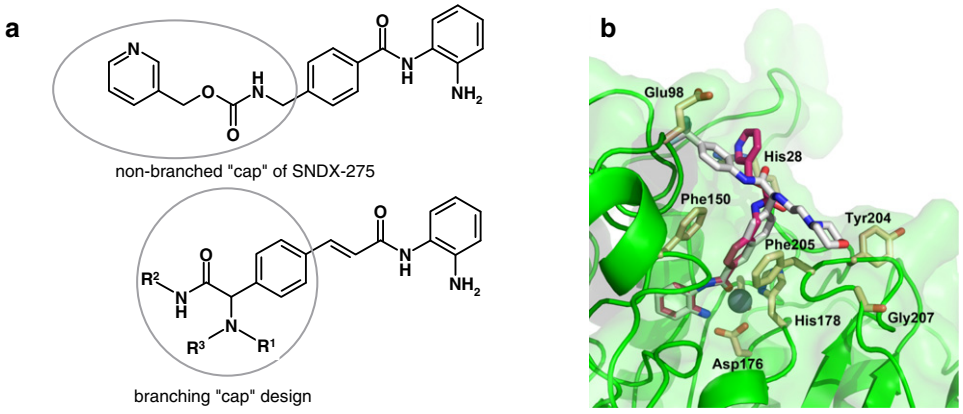

Figure 3. (a) Branching 'cap' design of novel 2-aminoanilides compared with non-branched cap-containing SNDX-275 and (b) overlay of representative novel 2-aminoanilide **5q** (white sticks) and non-branched clinical HDACi SNDX-275 (dark red sticks) in an HDAC1 homology model (green cartoon with selected residues in yellow sticks) based on the HDLP crystal structure.[20]

transfection efficiency.[18] To the best of our knowledge the report herein represents the first parallel use of both p21 and klf2 assays to assess HDAC inhibitor in-cell selectivity.[14]

In order to generate HDAC inhibitors with in-cell p21 versus klf2 selectivity, we initiated our molecular design around the non-hydroxamate 2-aminoanilide-based HDAC inhibitors. Since

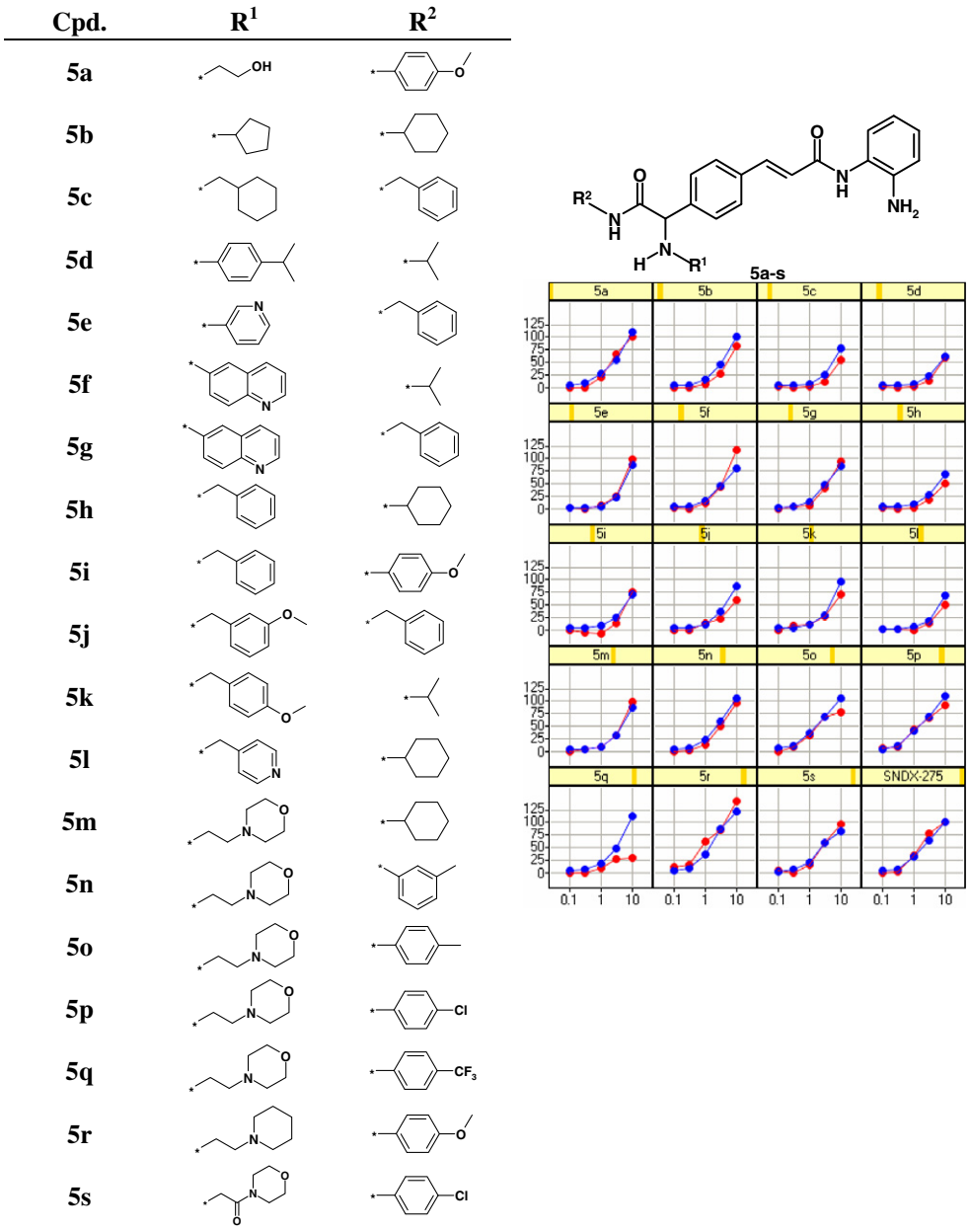

Figure 4. p21 (blue circles) and klf2 (red circles) induction curves for a representative set of 19 diverse α-aminoamides **5a**–**5s** relative to reference clinical 2-aminoanilide SNDX-275. *X*-axis is micromolar concentration in log scale; *Y*-axis is percent of the maximum induction observed for SNDX-275 (at 10 μM).

2-aminoanilides have essentially no activity toward HDAC6 or HDAC8 at either the enzymatic or in-cell level,[14,19] we felt that these substructures would provide a good starting point for achieving selectivity in our p21–klf2 screening system. We also introduced a branching point in the 'cap' portion of our molecules to increase their contact with the HDAC protein surface surrounding the entrance to the active site and also their likelihood of interacting with HDAC protein partners (Fig. 3a). Overlay of one of our designed 'branched cap' molecules (**5q**) and a non-branched clinical 2-aminoanilide SNDX-275 in an HDAC1 homology model illustrate this design concept (Fig. 3b). By combining the inherently selective 2-aminoanilide substructure with a branched capping group, we hoped to identify molecules with greater in-cell selectivity toward p21 versus klf2 compared to the existing non-branched 2-aminoanilides in clinical development such as SNDX-275 and MGCD0103 (Fig. 1).

The designed compounds were synthesized from a common intermediate, alpha-hydroxy ester **1** (Scheme 1).[18] Briefly, compound **1** was reacted with methanesulfonyl chloride at 0 °C in dichloromethane to obtain mesylate **2**. Mesylate displacement with various primary and secondary amines followed by one-pot hydrolysis of the ester and Boc-protection of the amine (in the case of secondary amino esters) gave amino acids **3**. Standard amide coupling with various amines gave amino amides **4**, which were then deprotected with methanolic HCl to obtain the final compounds **5**.

Final compounds were then evaluated for dose-dependent induction activity in both the aforementioned p21 and klf2 reporter gene assays. The results for a representative subset of the synthesized compounds (**5a–5s**) are shown (Fig. 4). Among the diverse set of R^1 and R^2 groups selected to decorate the cap portion of the α-aminoanilide analogues, the combination of an aromatic R^2 group with an aliphatic R^1 group containing a hydrogen bond acceptor connected via a two-atom linker (**5a**, **5n–5r**) provided consistently robust p21 induction. To our satisfaction, one

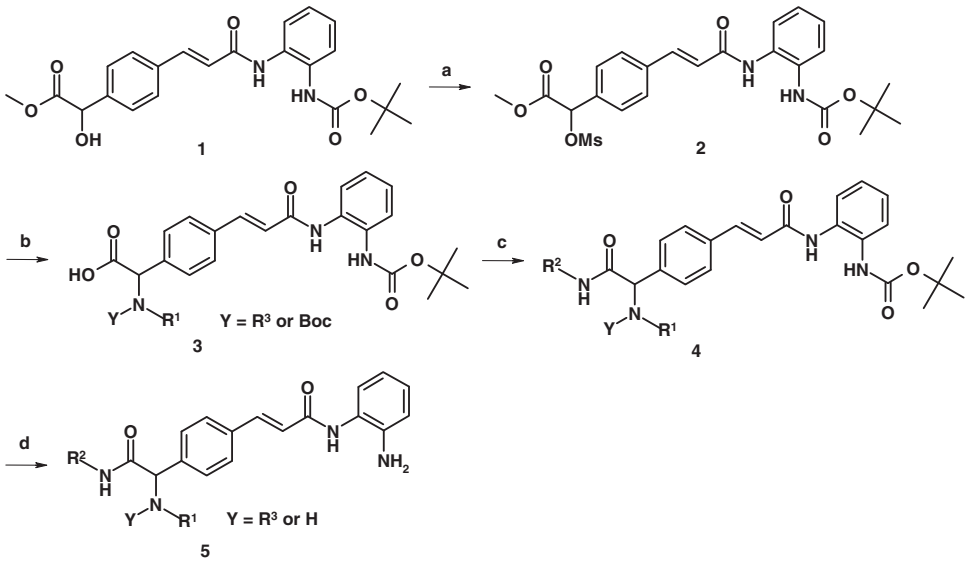

Scheme 1. General synthesis of α-amino amide 2-aminoanilides. (a) Triethylamine (1.5 equiv), CH_2Cl_2 at 0 °C, then MsCl (1.3 equiv), 1 h (>98% yield); (b) R^1YNH (Y = H or R^3), K_2CO_3, CH_3CN, 40 °C stir O/N then cool to rt; if Y = H then add 1 N LiOH, stir 5 h, then add Boc_2O, stir O/N (75% yield); if Y = R^3, then add 1 N LiOH, stir 5 h; (c) PyBrOP (2 equiv), DIPEA (2 equiv), CH_2Cl_2 then add R^2NH_2 (2 equiv) and stir O/N at rt; (d) 1.25 M HCl/CH_3OH stir O/N at rt (56% over two steps).

Table 1
Systematic exploration of the amino substituent (-NR^1R^3) compared to selective lead **5q**

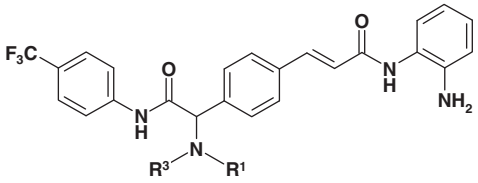

Compd	-NR^1R^3	p21 (RP3)[a] (%)	klf2 (RP3)[a] (%)	p21/klf2 (3 μM)[b]	p21 (RP10)[c] (%)	klf2 (RP10)[c] (%)	p21/klf2 (10 μM)[d]
5q	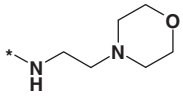	**86**	64	1.4	116	38	3.1
5t		31	32	1.0	73	40	1.8
5u		24	45	0.5	43	33	1.3
5v		**85**	62	1.4	89	69	1.3
5w	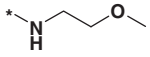	36	45	0.8	64	56	1.1
5x	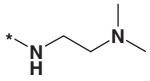	**138**	69	2.0	134	93	1.4
5y	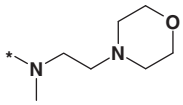	**72**	70	1.0	121	82	1.5
5z	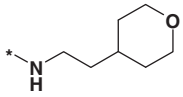	53	55	1.0	64	58	1.1
5aa	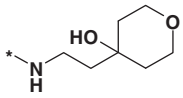	55	64	0.9	96	68	1.4
5ab	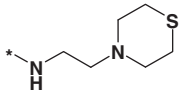	**71**	77	0.9	95	63	1.5

(*continued on next page*)

Table 1 (*continued*)

Compd	-NR[1]R[3]	p21 (RP3)[a] (%)	klf2 (RP3)[a] (%)	p21/klf2 (3 μM)[b]	p21 (RP10)[c] (%)	klf2 (RP10)[c] (%)	p21/klf2 (10 μM)[d]
5ac	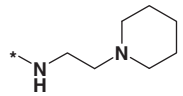	**163**	69	2.4	77	85	0.9
5ad	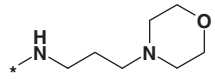	**139**	73	1.9	130	79	1.7
5ae	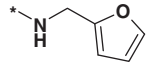	19	30	0.6	36	21	1.7

Blue-highlighted values are at or above the minimal desired induction activity for p21.
[a] RP3 is the percent induction activity of the listed analogue compared to SNDX-275 at 3 μM.
[b] This is the p21 RP3 value for the listed analogue divided by the klf2 RP3 value for the same analogue.
[c] RP10 is the percent induction activity of the listed analogue compared to SNDX-275 at 10 μM.
[d] This is the p21 RP10 value for the listed analogue divided by the klf2 RP10 value for the same analogue.

Table 2
Identification of additional analogues with selectivity toward p21 over klf2

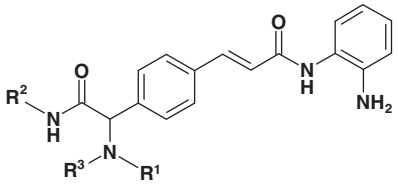

Compd	-NR[1]R[3]	-R[2]	p21 (RP3) (%)	klf2 (RP3) (%)	p21/klf2 (3 μM)	p21 (RP10) (%)	klf2 (RP10) (%)	p21/klf2 (10 μM)
5af	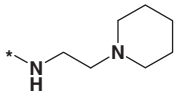	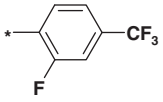	110	65	1.7	153	84	1.8
5ag	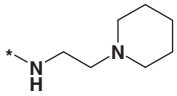	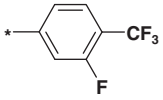	77	32	2.4	92	54	1.7
5ah	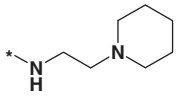	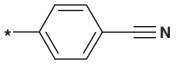	128	72	1.8	157	92	1.7
5ai	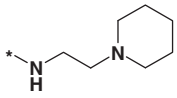	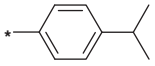	77	42	1.8	130	63	2.1
5aj	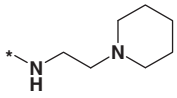	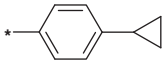	143	65	**2.2**	187	90	**2.1**
5ak	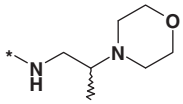	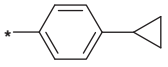	161	75	**2.2**	196	98	**2.0**
5al	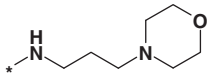	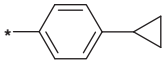	117	70	1.7	178	95	1.9
5am		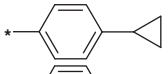	100	58	1.7	148	98	1.5
5an	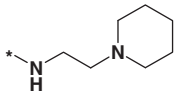	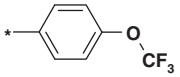	112	39	**2.9**	136	40	**3.4**
5ao	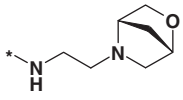	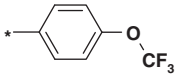	98	39	**2.6**	152	63	**2.4**

Table 2 (*continued*)

Compd	-NR^{1}R^3	-R^2	p21 (RP3) (%)	klf2 (RP3) (%)	p21/klf2 (3 μM)	p21 (RP10) (%)	klf2 (RP10) (%)	p21/klf2 (10 μM)
5ap	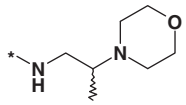	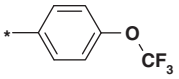	160	72	**2.2**	104	44	**2.4**
5aq	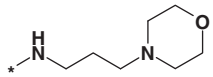	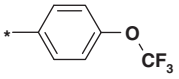	83	38	**2.2**	144	58	**2.5**
5ar	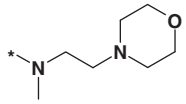	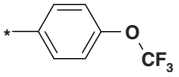	61	39	1.6	109	71	1.5
5as	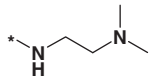	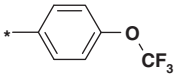	152	85	1.8	182	74	2.5

p21/klf2 ratios highlighted in blue showed similar selectivity to lead **5q**.

Table 3
Antiproliferative effect of selective analogues toward HeLa and A204 cells after 24 h treatment

Compd	%HeLa Growth (24 h)[a]		%A204 Growth (24 h)[a]	
	3 μM	10 μM	3 μM	10 μM
5aj	103	81	93	89
5an	105	61	95	88
5ao	103	82	97	90
5ap	107	83	97	93

[a] Percent growth compared to vehicle-treated control cells.

Table 4
HDAC1, 2, and 3 enzyme selectivity data for selected compounds

Compd	IC50 (μM)[a]		
	HDAC1	HDAC2	HDAC3
SNDX-275	0.6	1	1
5q	0.06	0.29	0.46
5aj	0.05	0.24	0.36
5z	0.2	0.8	1

[a] Enzyme IC_{50}s were determined by Reaction Biology Corp. (www.reactionbiology.com).

Table 5
Antiproliferative activity of lead **5q** in several representative cancer cell lines

Cell line	Cancer type	**5q** GI_{50} (μM, 72 h)
HeLa	Cervical	2.2
U2OS	Osteosarcoma	1.0
HepG2	Liver	1.7
MCF-7	Breast	1.9
HL-60	Leukemia	0.4
HCT-116	Colon	1.0

GI_{50} values were determined by 72 h tetrazolium dye assay using half-log serial dilutions from 30 μM to 100 nM compound concentration. Assay was performed according to previously published protocols based on assay kit instructions.[18]

of these relatively potent p21 inducers (**5q**), containing a 4-trifluoromethyl-substituted phenyl R^2 group, had significant selectivity toward p21 induction over klf2 induction.

Based on the promising selectivity result obtained with α-aminoanilide **5q**, we synthesized a series of **5q** analogues, focusing on systematic structural variations to investigate the structure–selectivity relationship. We began by fixing the 4-trifluoromethyl substituted phenyl group and varying the α-amino substituent to obtain compounds **5t–5ae** (Table 1). Within this subseries, it was apparent that good p21 activity generally required a moderately basic amine attached via a short hydrocarbon spacer to the α-amino group, as illustrated by compounds **5x**, **5y**, **5ab–5ad** (blue-highlighted values showing compounds with at least 70% p21 induction relative to SNDX-275). In addition, the pyrrolidine analogue **5v** also had good p21 activity, possibly due to conformational restriction introduced by the more sterically hindered tertiary amine. Among the analogues with good p21 activity, several showed hints of p21/klf2 selectivity at 3 μM, although at higher concentrations this selectivity was not maintained. Nevertheless, the structural trends for p21 activity observed among these analogues helped to narrow the selection of α-amino substituents during the exploration of aromatic R^2 groups to obtain additional compounds with selectivity toward p21 over klf2.

Variation of the aromatic R^2 group in our α-aminoamide series led to the identification of several new analogues with p21/klf2 selectivity (Table 2). Notably, compounds containing the 4-cyclopropyl and 4-trifluoromethoxy substituents combined with the previously identified amino substituents (**5aj**, **5ak**, **5an**–**5aq**) showed similar selectivity to the original lead **5q**, thus outlining a preliminary SAR space for further optimization.

In order to demonstrate that the observed p21/klf2 selectivity was not due to greater antiproliferative efficacy toward A204 cells versus HeLa cells (thus artificially decreasing the klf2 reporter gene signal), we evaluated the effect of representative selective analogues on A204 and HeLa cell growth after 24 h treatment (longer than the actual reporter gene assay treatment time but shorter than the typical 72 h cell proliferation assay). To our satisfaction, the results of this experiment (Table 3) showed that p21/klf2-selective analogues did not show significantly different antiproliferative effects in HeLa cells versus A204 cells within the timeframe of the reporter gene assays. Therefore, the observed selectivity of our novel 2-aminoanilides toward p21 induction over klf2 induction is not due to differential antiproliferative effects between the two respective cell lines (HeLa and A204) used for the reporter gene assays.

We were curious to know whether the selectivity of our 2-aminoanilides in the p21/klf2 reporter gene system could be due to differences in selectivity at the enzyme level. We therefore assessed the enzymatic selectivity of a representative set of these in-cell selective compounds, particularly toward the relevant subtypes HDAC1-3 (Table 4). Compared with SNDX-275, our p21/klf2-selective analogues (**5q** and **5aj**) showed about 10-fold greater potency toward HDAC1, 3–4-fold higher potency versus HDAC2, but only moderately higher potency (less than threefold) versus HDAC3. In contrast, the non-selective tetrahydropyran analogue **5z** (missing the basic amine

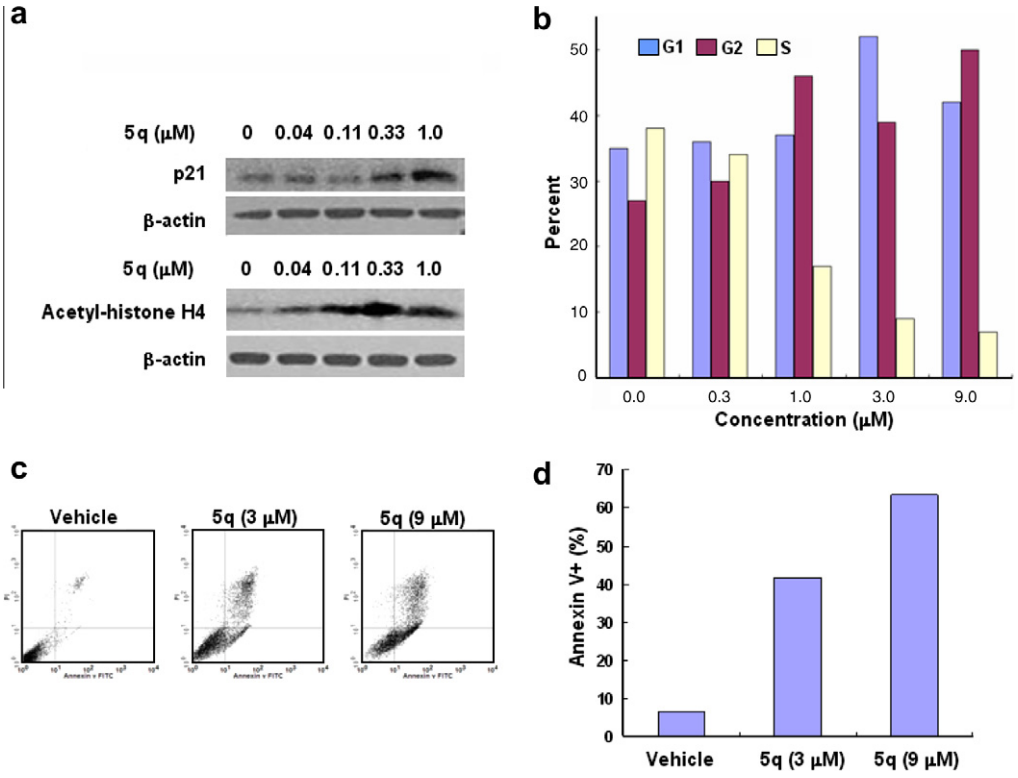

Figure 5. (a) Dose-dependent induction of acetylated histone H4 and endogenous p21 by **5q** in HCT-116 cells after 24 h treatment; (b) dose-dependent cell cycle arrest in HCT-116 cells treated with various concentrations of **5q** after 24 h treatment; (c) dose-dependent induction of apoptosis by **5q** versus vehicle at 48 h in HCT-116 cells as assessed by annexin V positivity in FACS analysis; (d) percent annexin V staining positivity in bar chart format for **5q** at 48 h in HCT-116 cells.

important for good p21 activity) was only moderately more potent than SNDX-275 toward HDAC1 (about threefold) and similar in potency to SNDX-275 toward HDAC2 and HDAC3. Taken together, these enzyme inhibition data suggest that the p21/klf2 selectivity of our 2-aminoanilides may in part be correlated to a distinct enzyme selectivity profile compared to clinical 2-aminoanilides such as SNDX-275. Further investigation will be required to fully elucidate the molecular origin of the in-cell selectivity of our branched 2-aminoanilide HDAC inhibitors.

Finally, in order to demonstrate the potential relevance of our novel 2-aminoanilides to cancer therapy, we evaluated the antiproliferative efficacy of lead compound **5q** in a panel of cancer cell lines (Table 5) via 72 h tetrazolium dye cell proliferation assay. The GI_{50} values for **5q** in this panel were in the low single-digit micromolar range. In particular, the antiproliferative activity of **5q** in HCT-116 colon cancer cells was also shown to be associated with induction of acetylated histone H4, endogenous p21, classical G_1/G_2 cell cycle arrest (with dose-dependent decrease in S phase population) and apoptosis (as assessed by annexin V positivity) (Fig. 5) in the same cell line. Taken together, the induction of classical in-cell markers of HDAC inhibition (acetylated histone H4 and p21) along with corresponding functional effects on the HCT-116 cancer cells provide in vitro evidence for the utility of **5q** and related analogues for cancer therapy.

In conclusion, we have discovered a novel series of 2-aminoanilide HDAC inhibitors which selectively induce p21 over klf2 relative to the clinical reference compound SNDX-275 in reporter gene-based selectivity assays. A representative lead from this series, **5q**, showed promising in vitro anticancer activity associated with induction of acetylated histone H4, endogenous p21, cell cycle arrest, and apoptosis. This lead series represents a viable starting point for the identification of a clinically-differentiated HDAC inhibitor for cancer therapy.

Acknowledgments

The authors would like to thank the Roche R&D Center (China) Ltd analytical, purification, and compound management teams for their invaluable support of this research.

References and notes

1. Prives, M.; Manley, J. L. *Cell* **2001**, *107*, 815.
2. Kovacs, J. J.; Murphy, P. J. M.; Gaillard, S.; Zhao, X.; Wu, J.-T.; Nicchitta, C. V.; Yoshida, M.; Toft, D. O.; Pratt, W. B.; Yao, T.-P. *Mol. Cell* **2005**, *18*, 601.
3. Kawaguchi, Y.; Kovacs, J. J.; McLaurin, A.; Vance, J. M.; Ito, A.; Yao, T.-P. *Cell* **2003**, *115*, 727.
4. Jin, Y.-H.; Jeon, E.-J.; Li, Q.-L.; Lee, Y. H.; Choi, J.-K.; Kim, W.-J.; Lee, K.-Y.; Bae, S.-C. *J. Biol. Chem.* **2004**, *279*, 29409.
5. Qian, D. Z.; Kachhap, S. K.; Collis, S. J.; Verheul, H. M.; Carducci, M. A.; Atadja, P.; Pili, R. *Cancer Res.* **2006**, *66*, 8814.
6. Hassig, C. A.; Schreiber, S. L. *Curr. Opin. Chem. Biol.* **1997**, *1*, 300.
7. Luo, J.; Su, F.; Chen, D.; Shiloh, A.; Gu, W. *Nature* **2000**, *408*, 377.
8. Oehme, I.; Deubzer, H. E.; Wegener, D.; Pickert, D.; Linke, J.-P.; Hero, B.; Kopp-Schneider, A.; Westermann, F.; Ulrich, S. M.; von Deimling, A.; Fischer, M.; Witt, O. *Clin. Cancer Res.* **2009**, *15*, 91.
9. Bolden, J. E.; Peart, M. J.; Johnstone, R. W. *Nat. Rev. Drug Disc.* **2006**, *5*, 769.
10. Yang, X.-J.; Seto, E. *Nat. Rev. Mol. Cell Biol.* **2008**, *9*, 206.
11. Grozinger, C. M.; Schreiber, S. L. *Chem. Biol.* **2002**, *9*, 3.
12. Haggarty, S. J.; Koeller, K. M.; Wong, J. C.; Grozinger, C. M.; Schreiber, S. L. *Proc. Natl. Acad. Sci. U.S.A.* **2003**, *100*, 4389.
13. Miller, T. A.; Witter, D. J.; Belvedere, S. *J. Med. Chem.* **2003**, *46*, 5097.
14. Wong, J. C.; Hong, R.; Schreiber, S. L. *J. Am. Chem. Soc.* **2003**, *125*, 5586.
15. Huang, L.; Sowa, Y.; Sakai, T.; Pardee, A. B. *Oncogene* **2000**, *19*, 5712.
16. Wilson, A. J.; Byun, D. S.; Popova, N.; Murray, L. B.; L'Italien, K.; Sowa, Y.; Arango, D.; Velcich, A.; Augenlicht, L. H.; Mariadason, J. M. *J. Biol. Chem.* **2006**, *281*, 13548.
17. Kumar, A.; Lin, Z.; SenBanerjee, S.; Jain, M. K. *Mol. Cell. Biol.* **2005**, *25*, 5893.
18. Chen, L.; He, Y.; Wong, J. C. PCT Int. Appl., WO2009095324, 2009.
19. For example, prototypical 2-aminoanilide MGCD0103 has IC_{50}s greater than 30 μM for HDAC6 and HDAC8.
20. Finnin, M. S.; Donigian, J. R.; Cohen, A.; Richon, V. M.; Rifkind, R. A.; Marks, P. A.; Breslow, R.; Pavletich, N. P. *Nature* **1999**, *401*, 188.